The Vibrational Spectrum and Ultimate Modulus of Polyethylene

Gustavo D. Barrera

Departamento de Química, Universidad Nacional de la Patagonia SJB, Ciudad Universitaria, 9005 Comodoro Rivadavia, Argentina

Stewart F. Parker* and Anibal J. Ramirez-Cuesta

ISIS Facility, Rutherford Appleton Laboratory, Chilton, Didcot, Oxon OX11 0QX, U.K.

Philip C. H. Mitchell

School of Chemistry, University of Reading, Reading, RG6 6AD, U.K.

Received December 5, 2005; Revised Manuscript Received February 8, 2006

ABSTRACT: We have performed the first completely ab initio lattice dynamics calculation of the full orthorhombic cell of polyethylene using periodic density functional theory in the local density approximation (LDA) and the generalized gradient approximation (GGA). Contrary to current perceptions, we show that LDA accurately describes the structure whereas GGA fails. We emphasize that there is no parametrization of the results. We then rigorously tested our calculation by computing the phonon dispersion curves across the entire Brillouin zone and comparing them to the vibrational spectra, in particular the inelastic neutron scattering (INS) spectra, of polyethylene (both polycrystalline and aligned) and perdeuteriopolyethylene. The Γ-point frequencies (where the infrared and Raman active modes occur) are in good agreement with the latest low temperature data. The near-perfect reproduction of the INS spectra, gives confidence in the results and allows us to deduce a number of physical properties including the elastic moduli, parallel and perpendicular to the chain. We find that the Young's modulus for an infinitely long, perfectly crystalline polyethylene is 360.2 GPa at 0 K. The highest experimental value is 324 GPa, indicating that current high modulus fibers are ∼90% of their maximum possible strength.

Introduction

Polyethylene $-(CH_2-CH_2)_n-$ is the largest tonnage plastic; in 2005 worldwide production was ca. 60000000 tons. It has been produced commercially since 1939 for a wide range of applications from electrical insulation to packaging and pipes. Its usefulness derives from its low cost, that it is easy to process, its chemical resistance and the ability to tailor its properties by the method of manufacture and the inclusion of comonomers (usually *n*-alk-1-enes, where $n = 3-12$).[1]

Chemically, polyethylene is the simplest possible polymer; however, the apparent simplicity of the molecular formula $(CH_2)_n$ belies the real complexity of the material. To understand the physical properties of the polymer, it is necessary to consider at least a two-phase model consisting of crystalline blocks in an amorphous matrix.[2] The crystalline component ranges from ca. 50% to >95%, generally it increases with increasing molecular weight and decreases with increasing chain branching. High performance fibers are obtained from ultrahigh molecular weight polymer, by processing so that the polymer chains are extended and aligned as in the crystalline material. The performance is improved as the chain length and crystallinity are improved.[3]

The elastic modulus of such fibers can exceed that of steel.[3] The ultimate modulus of these materials is of enormous interest for engineering applications and as a standard to measure existing materials against. As such, the modulus has been the subject of extensive experimental (mechanical,[4] X-ray diffraction,[5−7] coherent inelastic neutron scattering (INS),[8] Raman spectroscopy[9−11]), and theoretical (empirical[12] and Hartree−Fock[13] derived force fields, ab initio molecular dynamics[14]) investigations. Unfortunately there is no agreement as to the true value; estimates range from 210 to 358 GPa.

The modulus depends on the strength of the bonds in the polymer; these also determine the vibrational frequencies. Thus, a calculation that can reproduce both the structure *and* dynamics of polyethylene would provide a reliable value for the modulus. While this idea has been used before, comparison with the vibrational frequencies is usually only done for the Γ point (Brillouin zone center) frequencies. Polyethylene has significant dispersion in many of its modes,[15] so a comparison that accesses all of the Brillouin zone would be a much more exacting test of the calculation. In contrast to infrared and Raman spectroscopies that only observe modes at the Γ point, the mass of the neutron means that inelastic neutron scattering (INS) spectroscopy accesses the complete Brillouin zone.[16]

In this paper we have performed the first completely ab initio lattice dynamics calculation of the full orthorhombic cell of polyethylene. We emphasize that there is no parametrization of the results. We describe the calculation and show that it accurately reproduces the structure. We then test it by comparison to the previously reported INS spectra of polyethylene (polycrystalline and aligned)[17] and perdeuteriopolyethylene.[18−22] The near-perfect reproduction of the INS spectra, gives confidence in the results and allows us to deduce a number of physical properties including the elastic moduli, parallel and perpendicular to the chain.

Theoretical Methods

In the quasiharmonic approximation,[23] it is assumed that the Helmholtz energy of a crystal, *F*, at temperature *T* is the sum of static and vibrational contributions:

* To whom correspondence should be addressed. E-mail: S.F.Parker@rl.ac.uk.

10.1021/ma052602e CCC: $33.50
Published on Web 03/08/2006

$$F = E_{\text{stat}} + F_{\text{vib}}(T) \tag{1}$$

Here E_{stat} is the potential energy of the static lattice in a given configuration and F_{vib} is the sum of the harmonic vibrational contributions from the normal modes. For a periodic structure, the frequencies $\omega_j(\mathbf{q})$ are obtained by diagonalization of the dynamical matrix,[24] so that F_{vib} is given by[23]

$$F_{\text{vib}} = \sum_{j=1}^{3N}\sum_{\mathbf{q}}\left(\frac{1}{2}\hbar\omega_j(\mathbf{q}) + kT\ln(1 - e^{-\hbar\omega_j/kT})\right) \tag{2}$$

where the first term is the zero-point energy at $T = 0$ and the second term is the thermal contribution. For a macroscopic crystal, the sum over $\mathbf{q}$ becomes an integral over a cell in reciprocal space, which can be evaluated by taking successively finer uniform grids until convergence is achieved. Vibrational frequencies do not depend on temperature explicitly, but do so implicitly through the position of the atoms in the unit cell, which determines the dynamical matrix $\mathbf{D}$. This is defined by

$$D^{\alpha\beta}_{\kappa_i\kappa_j}(\mathbf{q}) = \frac{1}{\sqrt{m_{\kappa_i}m_{\kappa_j}}}\sum_{l_j}\Phi_{\alpha\beta}\begin{pmatrix}0 & l_j\\ \kappa_i & \kappa_j\end{pmatrix}e^{i\mathbf{q}\cdot\mathbf{r}(l_j)} \tag{3}$$

The $\Phi_{\alpha\beta}\begin{pmatrix}0 & l_j\\ \kappa_i & \kappa_i\end{pmatrix}$ are second derivatives of the crystal energy with respect to atom coordinates:

$$\Phi_{\alpha\beta}\begin{pmatrix}0 & l_j\\ \kappa_i & \kappa_j\end{pmatrix} = \frac{\partial^2\Psi}{\partial x_\alpha\begin{pmatrix}0\\ \kappa_i\end{pmatrix}\partial x_\beta\begin{pmatrix}l_j\\ \kappa_j\end{pmatrix}} \tag{4}$$

The free energy obtained is a function of both some external coordinates, $\mathscr{R}^{\text{ext}}$, which are here taken as the lattice parameters and a set of internal coordinates which give the position of the atoms within the unit cell $\mathscr{R}^{\text{int}} = \{r\}$; this whole set of coordinates is denoted collectively as $\mathscr{R}$. For a given temperature and applied pressure, P_{ext}, the crystal structure is that which minimizes the availability $\tilde{G}$:[25]

$$\tilde{G}(\mathscr{R}) = F(\mathscr{R}) + P_{\text{ext}}V(\mathscr{R}^{\text{ext}}) \tag{5}$$

At the equilibrium configuration $P = P_{\text{ext}}$ and the availability equals the Gibbs energy:

$$\tilde{G} = G \equiv F + PV \tag{6}$$

An efficient method to minimize $\tilde{G}$ is described elsewhere.[26]

Polyethylene crystallizes in the orthorhombic space group $Pnam \equiv D_{2h}^{16}$ (number 62). The structure is primitive with four CH_2 groups (two chains) per unit cell. Both carbon and hydrogen atoms occupy the special symmetry positions 4*c* at (x, $^1/_4$, z) with different values of x and z for carbon and two inequivalent hydrogen atoms. There are then three external and six internal coordinates to be determined. Though presently available computational resources make it possible to minimize the static energy with respect to this set of nine coordinates, it is currently too costly to optimize the whole set of variables by carrying out fully dynamic optimizations. For several systems that include ionic solids,[27] metals,[28] and even polyethylene[29] with force field potentials, it has already been shown that the use of the zero internal stress static approximation[29] (ZSISA) is a very good approximation for the evaluation of properties such as free energies, enthalpies, entropies, heat capacities, and thermal expansion. In this approximation, only external strains are relaxed fully dynamically while internal degrees of freedom are relaxed in the static approximation. The use of ZSISA would then involve the minimization of $\tilde{G}$ with respect to the three lattice parameters a, b, and c. For each given set of external coordinates, the six internal coordinates are optimized in the static approximation, and the vibrational contributions are then evaluated for the configuration thus obtained.

Here it is important to emphasize the difference between static calculations, calculations at 0 K, and at finite temperature, for instance 20 K. Static calculations assume that atoms are fixed at their equilibrium positions, which are determined by minimizing the static energy E_{stat}. Vibrational contributions are not included. Calculations at $T = 0$ K require the evaluation of phonon frequencies and the minimization of $E_{\text{stat}} + \sum_{j=1}^{3N}\sum_{\mathbf{q}}1/2\hbar\omega_j(\mathbf{q})$. The difference between static and 0 K calculations involves the zero point energy contribution $\sum_{j=1}^{3N}\sum_{\mathbf{q}}1/2\hbar\omega_j(\mathbf{q})$. Although still commonly used in the literature, it is misleading to use the expression "calculations at 0 K" when referring to static calculations. Calculations at finite temperature involve the minimization of $E_{\text{stat}} + \sum_{j=1}^{3N}\sum_{\mathbf{q}}1/2\hbar\omega_j(\mathbf{q}) + kT\ln(1 - e^{-\hbar\omega_j/kT})$, including both the zero point energy and the thermal contribution $kT\ln(1 - e^{-\hbar\omega_j/kT})$.

Our calculations were carried out using plane wave density functional theory as implemented in the computer code Abinit.[30] Here, there are two main approximations. The first approximation is the use of *pseudopotentials* to represent the core electrons, allowing one to include relativistic effects in a mainly nonrelativistic code, and to reduce the number of planes waves necessary to represent the wave function to a number tractable with available computer power. The second approximation is inherent in the use of density functional theory. In the *local density approximation* (LDA), the exchange and correlation energies depend on the local density on each point in space. In the *generalized gradient approximation* (GGA), electron density gradients are taken into account to determine the exchange and correlation energies.[31] The LDA calculations were done using the Teter−Padé parametrization;[32] the GGA calculations were based on the parametrization of Perdew, Burke, and Ernzerhof.[33] We used the Troulliers and Martins pseudopotentials[34] as provided with Abinit.[30]

We have verified that convergence is achieved with respect to the number of k-points in reciprocal space and energy cutoff for the plane waves. Most calculations were done using a mesh of $2 \times 4 \times 8$ points in reciprocal space and a cutoff of 1360.6 eV. Phonon frequencies were calculated on a subgrid (of $1 \times 2 \times 4$ points of reciprocal space) of that used for the electronic structure calculations. More points in reciprocal space were generated for the calculation of the phonon frequencies by using the interpolation algorithm of Gonze as implemented in the Anaddb code.[35] From the phonon frequencies, free energies and derived thermodynamic properties were determined using standard lattice dynamics calculations in the quasiharmonic approximation as described above.

The intensity, S, of an INS spectral band is a function of both the energy, $\hbar\omega$, and the momentum, $\mathbf{Q}$, exchanged during the scattering process. Recalling that $|\mathbf{q}| = 2\pi/\lambda$ and $Q = |\mathbf{Q}|$, from conservation of momentum and energy we have

$$\mathbf{Q} = \mathbf{q}_{\text{scattered}} - \mathbf{q}_{\text{incident}} \tag{7}$$

$$\hbar\omega = E_{\text{tranf}} = E_{\text{incident}} - E_{\text{scattering}} = \frac{\hbar^2}{2m_n}(|\mathbf{q}_{\text{incident}}|^2 - |\mathbf{q}_{\text{scattering}}|^2) \tag{8}$$

where $\mathbf{q}_{\text{incident}}$ and $\mathbf{q}_{\text{scattered}}$ are the momentum of the neutron before and after the scattering process and E_{incident} and $E_{\text{scattering}}$ are the corresponding kinetic energies of the neutron. On the TFXA and TOSCA instruments[36] (where most of the data were recorded[17,18]), the final energy of the instrument is fixed to be 32 cm^{-1}. Because of the relatively large momentum transfer in the TFXA and TOSCA measuring range (0−4000 cm^{-1}) the projection of the momentum transfer maps uniformly into the first Brillouin zone.[16]

The intensity of an INS band, S_α, produced by atom α when vibrating at a frequency ω_i with amplitude U_i is

$$S_\alpha(Q,n\omega_i) = \frac{(Q\cdot U_i)^{2n}}{n!}\exp(-(Q\cdot U_T)^2)\cdot\sigma_\alpha \qquad (9)$$

where $n = 1$ for a fundamental mode, 2 for a first overtone or binary combination, 3 for a second overtone or ternary combination, and so forth; Q is the momentum transfer defined before, σ_α is the scattering cross section of atom α, U_i is the amplitude of the normal mode i and U_T is the total root-mean-square displacement of all the atoms in all the modes, both internal and external.

For a periodic solid, the solution of the vibrational problem contains a dependency with the wavevector in reciprocal space, the intensity is now:

$$S_\alpha(Q,n\omega_i) = \frac{1}{V_{\text{Brillouin}}}\int\frac{(Q\cdot U_i(\mathbf{q}))^{2n}}{n!}\exp(-(Q\cdot U_T)^2)\cdot\sigma_\alpha\, d\mathbf{q}^3 \qquad (10)$$

The integration has to be performed over the whole Brillouin zone; $V_{\text{Brillouin}}$ is the volume of the Brillouin zone. To calculate the INS spectra of polyethylene, we need a fine grid of points in the Brillouin zone, we used a 8 × 16 × 128 grid to obtain well-defined INS spectra. We do not need to undertake a full electronic calculation in such a grid, instead we make use of the Anaddb program from the package. The output of Abinit includes both the frequencies and the atomic displacements, from ref 16; these are what are needed for the generation of the INS spectrum, which was done using the ACLIMAX program.[36,37]

Results and Discussion

Structure. Previous[38,39] ab initio calculations of polyethylene using GGA found that the crystal is either unstable with respect to interchain separation or only exhibits a shallow energy minimum. Carrying out GGA using similar functional forms but with much more stringent convergence with respect to the number of plane waves and grid points in reciprocal space we found polyethylene to be stable, although it greatly overestimates the lattice parameters perpendicular to the chain direction as also found in ref 39. In contrast, the results using LDA are in good agreement with the experimental data. Figure 1 compares the ab initio structural parameters with experimental[40−42] data from neutron diffraction of perdeuteriopolyethylene (PE-D_4).

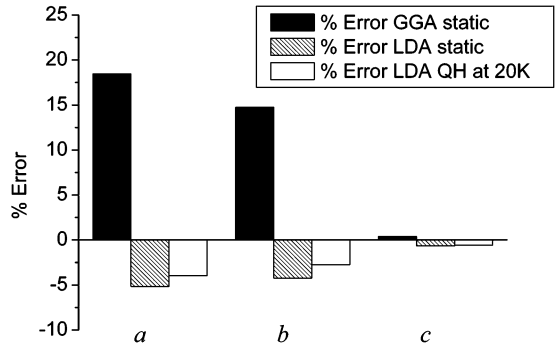

Figure 1. Error in the lattice parameters (relative to 4 K experimental data[40]) as a function of method.

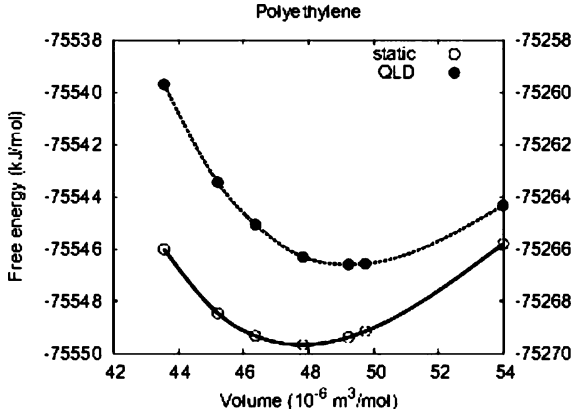

Figure 2. Free energy as a function of volume (left scale, solid circles) using the quasiharmonic approximation and the energies obtained in the static approximation at the same volumes (right scale, open circles).

As a further approximation, we optimize the whole set of coordinates for a set of pressures ranging from −1 to +2 GPa, in the static approximation and calculate, for each configuration, the corresponding vibrational contribution using lattice dynamics in the quasiharmonic approximation as explained above. In Figure 2, we show the free energies as a function of volume using this approximation of quasiharmonic lattice dynamics and the energies obtained in the static approximation. As expected, inclusion of the vibrational contributions increases the equilibrium volume from 4.779 × 10^{-5} to 4.924 × 10^{-5} m^3 mol^{-1}.

The importance of the quasiharmonic approximation is apparent; its use significantly reduces the error in the lattice parameters as shown in Figure 1. The geometry is in good agreement with the latest structural determination;[42] all of the calculated values are within the error bar of the corresponding experimental data, as shown in Table 1. We note that the bond distances and angles are all chemically reasonable. A comparison with structural data at low temperature would be preferable. Unfortunately, except for the work reported in ref 40, we are

Table 1. Comparison of Experimental and Ab Initio Structural Parameters

	a, Å	*b*, Å	*c*, Å	r_{CC}, Å	r_{CH}, Å	∠CCC, deg	∠HCH, deg	setting angle,[a] deg
GGA static	8.435	5.567	2.558					
LDA static	6.754	4.645	2.531					
LDA QH at 20 K PE-D_4	6.839	4.718	2.533	1.51	1.11	113.47	105.85	45.11
expt[40] 4 K PE-D_4	7.121	4.851	2.548	1.578(5)	1.06(1), 1.10(1)	107.7	109.0	41(1)
expt[41] 10 K PE-D_4	7.120	4.842						
expt[42] room temp PE-D_4	7.43	4.93	2.545	1.530(23)	1.099(45), 1.105(45)	112.6(2.1)	107.3(5.3)	42.4(3.3)

[a] The setting angle is the angle between the *ac* plane and the plane containing the C−C bonds of the polyethylene chain.

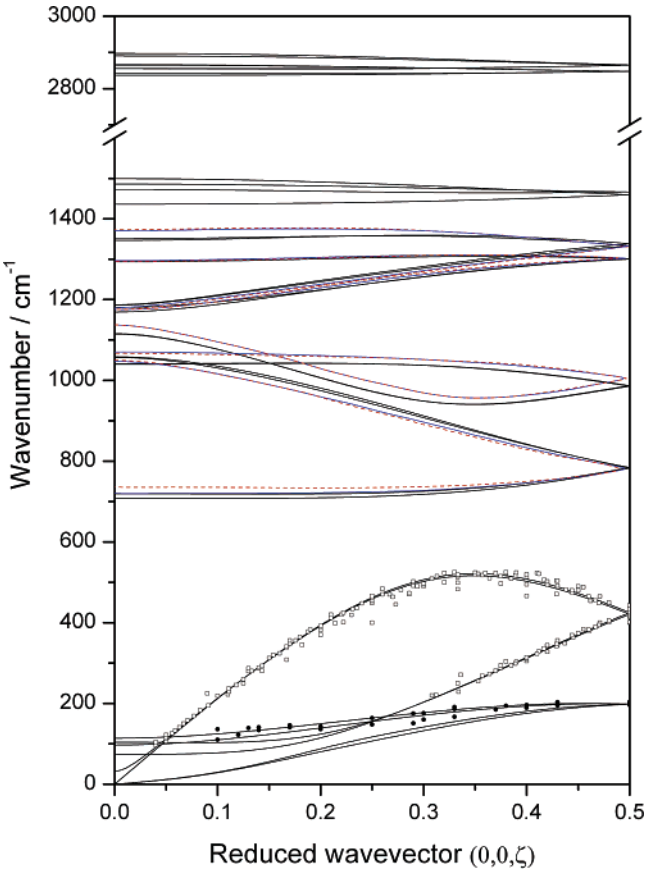

Figure 3. Comparison of the dispersion curves of hydrogenous polyethylene obtained in the present work (black lines) and those derived empirically from a force field model of the *n*-alkanes[44] (red lines). Also shown are the experimentally data for the longitudinal[47] (open squares) and transverse[48] (filled circles) acoustic modes.

not aware of any such data. Furthermore, the C−D, C−C, CCC, and ∠HCH values reported[40] are all distinctly different from conventional values. For this reason, we use the recent room-temperature data[42] for the comparison.

Dynamics. Dispersion curves of materials show the relation between the energy of a vibration and the wavevector k ($=2\pi/\lambda$, Å^{-1}) and are conventionally plotted over the first half of the Brillouin zone. In the case of a polymer, the dispersion curve can be plotted in two ways: either as a function of the phase difference θ between adjacent oscillators (for polyethylene these are CH_2 groups) or as a function of k, the phase difference between adjacent translational units. Since the unit cell of polyethylene contains two chain segments each consisting of two CH_2 groups, the cell is twice as long for the adjacent translational units as that for the adjacent oscillator and consequently the Brillouin zone of the former is half the size of the latter. Thus, dispersion curves as a function of k can be obtained from those as a function of θ by folding back the right-hand half of the plot. For infrared and Raman spectroscopy, the allowed modes are those at $k = 0$, the Brillouin zone center. In terms of θ the allowed modes are those at 0 and π since the dispersion curves in this case span a complete Brillouin zone, i.e., center-to-center. Equivalently, the selection rules require that vibrations in each translational unit are totally in phase. This is clearly satisfied at $\theta = 0$, but since the *all-trans* conformation of polyethylene is a 2_1 helix (one complete turn for each two chemical units) it follows that a phase difference of $\theta = \pi$ between adjacent oscillators will result in a phase difference of 2π between adjacent translational units and hence the $k = 0$ requirement is satisfied.

Dispersion curves of materials are usually measured experimentally by coherent INS.[43] ^{1}H has a large incoherent cross section (80.3 barn, 1 barn $= 10^{-28}$ m^{-2}) and a small coherent cross section (1.8 barn), so the incoherent scattering dominates the scattering and the coherent features are unobservable from hydrogenous materials. (Coherent INS is possible from perdeuterated polymers because the incoherent and coherent cross section's of ^{2}H are 2.0 and 5.6 barn, respectively. Perdeuteriopolyethylene is discussed later in this section.) Polyethylene is

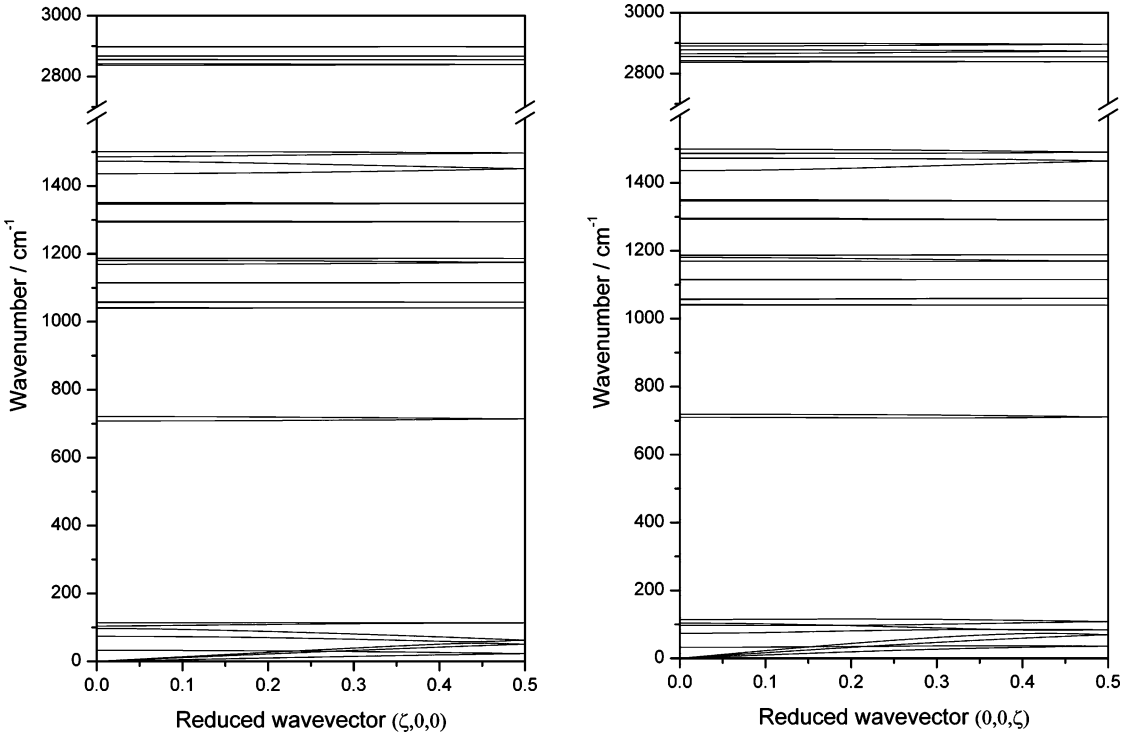

Figure 4. Calculated dispersion curves of hydrogenous polyethylene along the *a* (left) and *b* axes (right).

Table 2. Observed and Calculated Γ Point Frequencies of Polyethylene and Perdeuteriopolyethylene

		polyethylene		perdeuteriopolyethylene	
mode	symmetry	expt,[a] cm^{-1}	ab initio, cm^{-1}	expt[a], cm^{-1}	ab initio, cm^{-1}
$\nu_1^a(0)$	A_g	2846	2842	2103	2088
$\nu_1^b(0)$	B_{3g}		2837		2081
$\nu_1^a(\pi)$	B_{1u}	2850	2866	2095	2109
$\nu_1^b(\pi)$	B_{2u}		2865		2106
$\nu_2^a(0)$	A_g	1442	1436	970	970
$\nu_2^b(0)$	B_{3g}	1468	1472		989
$\nu_2^a(\pi)$	B_{1u}	1475	1500	1094	1106
$\nu_2^b(\pi)$	B_{2u}	1468	1486	1088	1096
$\nu_3^a(0)$	B_{3u}	1173	1185	890	897
$\nu_3^b(0)$	A_u		1187		898
$\nu_3^a(\pi)$	B_{2g}	1412	1351	1257	1207
$\nu_3^b(\pi)$	B_{1g}		1346		1206
$\nu_4^a(0)$	A_g	1134	1116	1149	1142
$\nu_4^b(0)$	B_{3g}		1114		1136
$\nu_4^a(\pi)$	B_{2g}	1062	1041	828	824
$\nu_4^b(\pi)$	B_{3g}		1040	824	821
$\nu_5^a(0)$	A_g	136	114	106	98
$\nu_5^b(0)$	B_{3g}	109	104	82	76
$\nu_5^a(\pi)$	B_{1u}	80	74	75	69
$\nu_5^b(\pi)$	B_{2u}	109	97	103	89
$\nu_6^a(0)$	A_g	2881	2855	2200	2073
$\nu_6^b(0)$	B_{3g}		2856		2071
$\nu_6^a(\pi)$	B_{1u}	2920	2897	2194	2145
$\nu_6^b(\pi)$	B_{2u}		2890		2141
$\nu_7^a(0)$	A_g	1172	1169	992	1014
$\nu_7^b(0)$	B_{2g}		1180		1025
$\nu_7^a(\pi)$	B_{2g}	1295	1293	917	915
$\nu_7^b(\pi)$	B_{1g}		1296		917
$\nu_8^a(0)$	B_{3u}	1050	1058	746	749
$\nu_8^b(0)$	A_u		1057		748
$\nu_8^a(\pi)$	B_{1u}	735	719	529	520
$\nu_8^b(\pi)$	B_{2u}	722	708	522	512
$\nu_9^a(0)$	B_{3u}		0		0
$\nu_9^b(0)$	A_u	53	32		30
$\nu_9^a(\pi)$	B_{1u}		0		0
$\nu_9^b(\pi)$	B_{2u}		0		0

[a] Experimental values at 4 K from refs 17, 18, and 49.

unique among polymers in that the homologous series of *n*-alkanes can considered as oligomers of polyethylene. The unit cell of the *n*-alkane contains the entire molecule, so the internal modes are allowed by the $k = 0$ selection rule. However, a subcell may be defined that only includes two CH_2 units (ignoring the methyl groups); the vibrations of these occur at subcell wavevectors that are integral multiples of the reciprocal oligomeric length; i.e., $0 \le k \le 1$. In this way, it is possible to map out the phonon dispersion curves of polyethylene along the chain axis (*c* direction) from the series of *n*-alkanes.[44] This has been done for the modes in the 700−1500 cm^{-1} region by infrared spectroscopy;[45] the modes below 700 cm^{-1} were characterized by Raman spectroscopy[46] and more recently by INS spectroscopy.[47,48]

Figure 3 shows the dispersion curves for protonated polyethylene from the present work and those derived empirically from a force field model of the *n*-alkanes.[44] Also shown are the experimental data for the longitudinal and transverse acoustic modes.[47,48] It can be seen that the agreement is almost quantitative across the entire range.

In the directions perpendicular to the chain axis, there are no experimental data. Figure 4 shows the calculated curves, and it can be seen that, apart from the acoustic modes, there is almost no dispersion in the modes. This is consistent with the weak intermolecular forces that are present.

The calculated Γ point frequencies of polyethylene are compared to the latest low-temperature infrared and Raman data[49] in Table 2. All of the gerade (g) modes are Raman active, the ungerade (u) modes are infrared active except for the A_u modes that are inactive in both forms of spectroscopy.

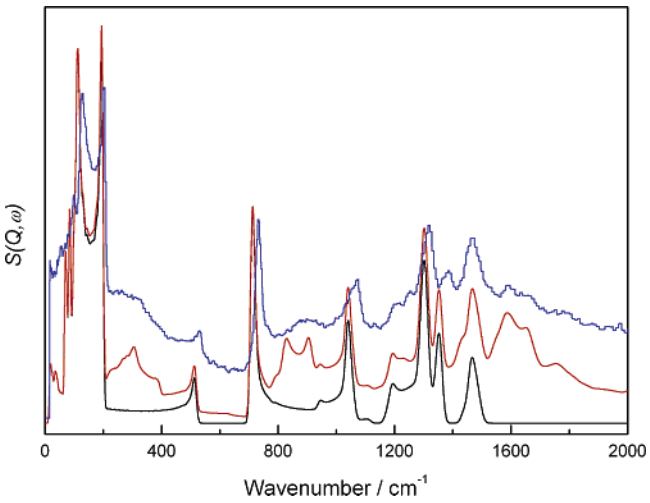

Figure 5. Comparison of the INS spectrum derived from the ab initio results: one-phonon modes only (black line), including all multiphonon processes up to and including $n = 10$, (red line) and that obtained from a polycrystalline sample of a high molecular weight linear polyethylene[17] (blue line).

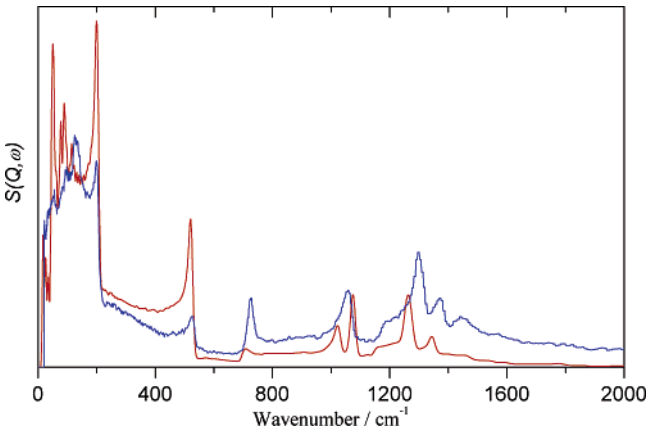

Figure 6. Comparison of observed[17] (blue) and ab initio (red) INS spectra of polyethylene with *Q* parallel to the *c* axis.

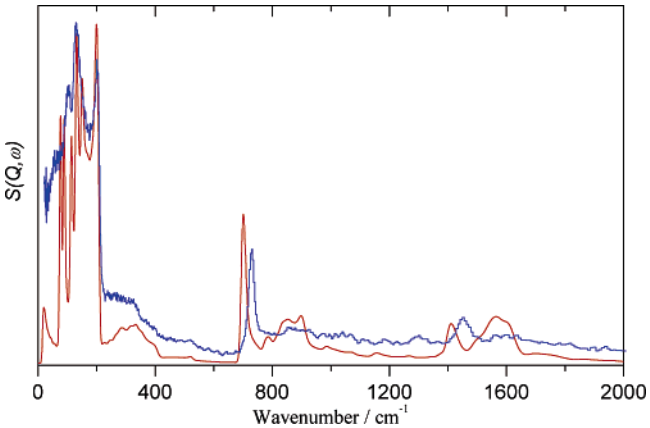

Figure 7. Comparison of observed[17] (blue) and ab initio (red) INS spectra of polyethylene with *Q* perpendicular to the *c* axis.

A more stringent test is to generate the INS spectrum and, as described in the Theoretical Methods, this can be done by properly sampling the Brillouin zone and using ACLIMAX.[37] The result is shown in Figure 5 and compared to that obtained from a polycrystalline sample of a high molecular weight linear polyethylene.[17] The agreement is again excellent. The double peak signature characteristic of polyethylene at ∼100 and ∼200 cm^{-1} is the result of the transverse acoustic modes, ν_9, at $\theta =$

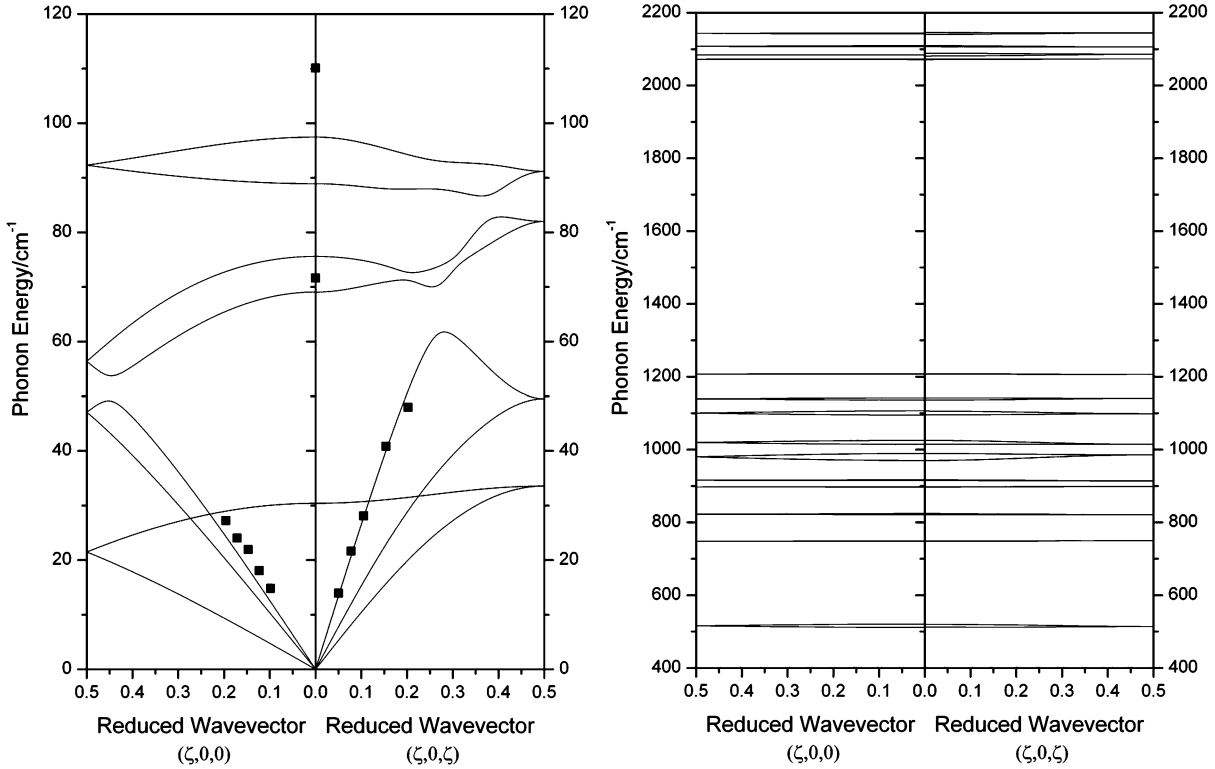

Figure 8. Comparison of ab initio dispersion curves (solid lines) and experimental data (points) for perdeuteriopolyethylene in the 0−120 cm^{-1} (left) and 400−2200 cm^{-1} regions (right).

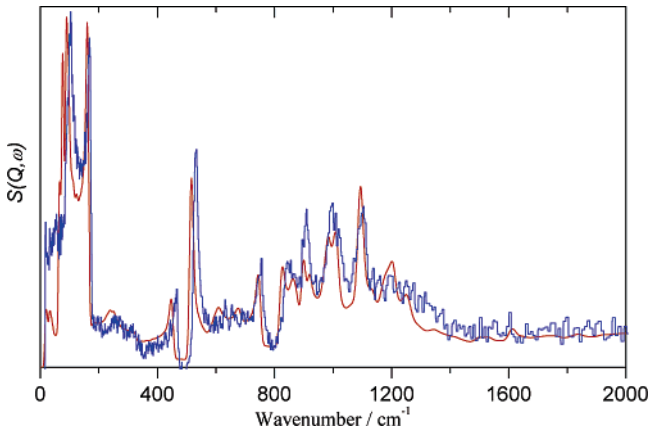

Figure 9. Comparison of the INS spectrum derived from the ab initio results (blue line) and that obtained from a polycrystalline sample of perdeuteriopolyethylene[18] (red line).

π and the maximum in ν_9 respectively. Comparison of the one phonon calculation (black line) with the multiphonon ($n \leq 10$, eq 9, red line) and experimental curves (blue line) shows that most of the intensity in the 200−550 cm^{-1} region is assignable to two phonon processes involving the transverse acoustic modes; the longitudinal acoustic modes contribute weakly and are only evidenced by the cutoff at 525 cm^{-1} resulting from the maximum in ν_5. At higher energies, the assignments are in agreement with those from a periodic calculation on a unit cell with a single chain.[50] This is to be expected since the dispersion curves in the *a* and *b* directions are almost flat, Figure 4, showing that in this region the two chains in the true unit cell are almost independent of each other, so a single chain provides a reasonable model.

A further test is provided by the comparison to drawn polyethylene[17] which results in a sample oriented along the *c* axis with a random alignment along the *a* and *b* directions. In this case the INS spectra depend on the orientation of the momentum transfer vector, *Q*, with respect to the *c* axis. Comparisons of the limiting cases with *Q* parallel to the *c* axis and perpendicular to the *c* axis are shown in Figures 6 and 7, respectively. In Figure 6, the agreement is not as good as expected, in particular the intensity of the feature at 720 cm^{-1}. As previously reported, we believe this to be the result of incomplete orientation in this direction, thus there is also a transverse component present.

Table 3. Observed and Calculated Elastic Constants (GPa) of Polyethylene

	this work	empirical[a]	ab initio[b]	expt[c]	expt[d]
C_{11}	15.95	13.3	41.18, 48.06	8.4	11.5
C_{12}	6.37	6.9	11.25, 12.21	4.2	
C_{13}	2.40	1.8	3.19, 1.43	5.5	
C_{22}	15.53	11.2	47.14, 44.22		
C_{23}	5.99	3.5	6.50, 6.20		
C_{33}	362.51	333.2	405.78, 375.19	102	290
C_{44}	6.16	4.0		1.81	
C_{55}	3.38	2.5			
C_{66}	6.02	6.1		2.02	
C_{110}^{L} [e]	12.6	9.6			14.2
$\bar{C}$[e]	12.1	9.7			6.5

[a] Reference 13. [b] Reference 53, calculated from LDA by two methods. [c] Reference 52. [d] Reference 8. [e] Defined in ref 8.

For perdeuteriopolyethylene, there are both more and less experimental data than for polyethylene. With perdeuteriopolyethylene it is possible to directly measure the dispersion curves using coherent INS.[19−22] However, this has only been achieved for the longitudinal and transverse acoustic modes below 550 cm^{-1}. The higher energy modes have not been mapped either directly by coherent INS or indirectly by using perdeuterioalkanes. Figure 8 compares the dispersion curves calculated in the present work with the experimental data. The calculated and observed Γ point frequencies are given in Table 2.

The calculated and observed[18] INS spectra of perdeuteriopolyethylene powder are compared in Figure 9. In all of Table

Table 4. Observed and Calculated Young's Moduli (GPa) of Polyethylene

	experimental				theoretical			
modulus	mechanical[4]	X-ray[5−7,54,]	Raman[9−11]	coherent INS[8]	ab initio[54]	molecular dynamics[14]	force field[12,13]	this work
Y_{cc}	288	235−255	280−358	329	350−400	334	286−386	360.20
Y_{bb}		2.5−5.0					9.4	12.92
Y_{aa}		1.9−3.9					9.0	13.34

2 and Figures 8 and 9 the agreement is excellent. The ab initio result was generated purely by using the mass of deuterium instead of hydrogen in the dynamical matrix, thus this is a harmonic calculation. The good agreement shows that polyethylene is largely a harmonic system.

Properties. The previous sections on Structure and Dynamics have demonstrated that our model is both accurate and reliable. In this section we calculate some of the properties including the Young's moduli. The bulk modulus (the reciprocal of the compressibility)is calculated as 15.65 GPa in the static approximation and 15.06 GPa in the quasiharmonic approximation. For low and high-density polyethylene, the experimental values at room temperature are 1.8[51] and 6.7[52] GPa, respectively.

Table 3 presents comparison of the observed and calculated elastic constants. The results from an empirical force field calculation[13] are in reasonable agreement with our ab initio results, with the empirical results generally 10−30% smaller than ours. This is in marked contrast to an ab initio calculation[53] where the values are much larger. The most comprehensive set of experimental values is from ultrasonic measurements[51] on a drawn high density polyethylene (Rigidex-50). There is poor agreement with these, with the experimental values generally only one-third to one-half of the ab initio results. There is better agreement with the less complete set obtained from coherent INS measurements of perdeuteriopolyethylene.[8]

The Young's modulus along the chain, Y_{cc}, is calculated as 360.20 GPa in the static approximation. The experimental results are generally smaller than this, but most of these were measured at room temperature and the modulus increases with decreasing temperature. The value of 288 GPa measured by a mechanical method at 77 K was extrapolated to 324 GPa at 0 K by the authors.[8] The more recent theoretical values are mostly in the range 330−360 GPa. The results indicate that the Young's modulus of the fibers used in for the mechanical test[4] have ∼90% of the maximum possible value.

Values for the Young's moduli perpendicular to the chain, Y_{aa} and Y_{bb}, are much larger than the experimental values[54] and somewhat larger than the force field derived values. The experimental values are again room-temperature measurements; the force field calculations indicate a decrease of about one-third between 0 and 300 K.

Conclusions

In previous papers, we have reported the structure and dynamics of the alkali metal hydrides (MH, M = Li, Na, K, Rb, Cs) calculated using both LDA and GGA.[55,56] Contrary to the currently perceived wisdom that, in general, GGA gives results in better agreement with experiment than does LDA, we found that the LDA results matched the experimental results, when thermodynamics is included using lattice dynamics for both the structure and dynamics, much better than the GGA results. The same pattern is seen in the present case with LDA giving results in better agreement with the experimental data than GGA, as demonstrated in Figure 1.

Almost all of the mechanical properties we calculate, bulk modulus, elastic constants and Young's moduli, are significantly larger than the experimental values. We believe that this is a reflection of the difficulty of the experimental measurements but, more importantly, the comparison is between the real material which is partly amorphous and our model which is 100% crystalline. We note that low and high density polyethylenes are usually only ∼60 and ∼80% crystalline and that the perdeuteriopolyethylene used for the coherent INS measurements[22] was no more than 75% crystalline. Since the mechanical strength of the amorphous region is less than that of the crystalline region, it would be expected that the ab initio results are consistently larger than the experimental values.

Our value for the Young's modulus along the chain, Y_{cc} = 360.20 GPa, is in general agreement with recent calculations[14,53] using ab initio methods. We have particular confidence in our result because we have validated our results by comparison to the vibrational spectra. The modulus will largely depend on the force constants for C−C stretch and C−C−C bending and from Figure 2 and Table 2, both of these are well described across the entire Brillouin zone.

Acknowledgment. The Rutherford Appleton Laboratory is thanked for access to neutron beam facilities. The CCLRC Centre for Molecular Structure and Dynamics (CMSD) is thanked for financial support for G.D.B.

References and Notes

(1) Mills, N. J. *Plastics: Microstructure and Engineering Applications*; Edward Arnold: Bury St. Edmunds, U.K., 1993.
(2) Young, R. J.; Lovell, P. A. *Introduction to Polymers*; Chapman: London, 1991.
(3) Crist, B. *Annu. Rev. Mater. Sci.* **1995**, *25*, 295.
(4) Barham, P. J.; Keller, A. *J. Polym. Sci., Polym. Lett. Ed.* **1979**, *17*, 591.
(5) Sakurada, I.; Nukushina, Y.; Ito, T. *J. Polym. Sci.* **1962**, *57*, 651.
(6) Matsuo, M.; Sawatari, C. *Macromolecules* **1986**, *10*, 2036.
(7) Nishino, T.; Ohkubo, H.; Nakramae, K. *J. Macromol. Sci.—Phys.* **1992**, *B31*, 191.
(8) Twistleton, J. F.; White, J. W.; Reynolds, P. A. *Polymer* **1982**, *23*, 578.
(9) Shaufele, R. F.; Shimanouchi, T. *J. Chem. Phys.* **1967**, *47*, 3605.
(10) Strobl, G. R.; Eckel, R. *J. Polym. Sci., Polym. Phys. Ed.* **1976**, *14*, 913.
(11) Pietralla, M.; Hotz, R.; Siems, R. *J. Polym. Sci., Polym. Phys. Ed.* **1997**, *35*, 47.
(12) Palmö, K.; Krimm, S. *J. Polym. Sci., Polym. Phys. Ed.* **1996**, *34*, 37.
(13) Karasawa, N.; Dasgupta, S.; Goddard, W. A., III. *J. Phys. Chem.* **1991**, *95*, 2260.
(14) Hageman, J. C. L.; Neier, R. J.; de Groot, R. A. *Macromolecules* **1997**, *30*, 5953.
(15) Bower, D. I.; Maddams, W. F. *The Vibrational Spectroscopy of Polymers* Cambridge University Press: Cambridge, U.K., 1989.
(16) Mitchell, P. C. H.; Parker, S. F.; Ramirez-Cuesta, A. J.; Tomkinson, J. *Vibrational Spectroscopy with Neutrons, with Applications in Chemistry, Biology, Materials Science and Catalysis*; World Scientific: Singapore, 2005.
(17) Parker, S. F. *J. Chem. Soc., Faraday Trans.* **1996**, *92*, 1941.
(18) Parker, S. F. *Macromol. Symp.* **1997**, *119*, 227.
(19) Feldkamp, L. A.; Vankataraman, G.; King, J. S. *Neutron Inelastic Scattering*; International Atomic Energy Authority: Vienna, 1968; Vol. 2, p 159.
(20) Twistleton, J. F.; White, J. W. *Neutron Inelastic Scattering*; International Atomic Energy Authority: Vienna, 1972; p301.
(21) Pepy, G.; Grimm, H. *Neutron Inelastic Scattering*; International Atomic Energy Authority: Vienna, 1978; Vol. 1, 607.
(22) Holliday, L.; White, J. W. *Pure Appl. Chem.* **1971**, *26*, 545.
(23) Wallace, D. C. *Thermodynamics of Crystals*; Wiley: New York, 1972.

(24) Allan, N. L.; Barrera, G. D.; Fracchia, R. M.; Lavrentiev, M. Yu.; Taylor, M. B.; Todorov, I. T.; Purton, J. A. *Phys. Rev. B* **2001**, *63*, 094203.
(25) Pippard, A. B. *The Elements of Classical Thermodynamics.* Cambridge University Press: Cambridge, U.K., 1964.
(26) Taylor, M. B.; Barrera, G. D.; Allan, N. L.; Barron, T. H. K.; Mackrodt, W. C. *Comput. Phys. Commun.* **1998**, *109*, 135.
(27) Taylor, M. B.; Barrera, G. D.; Allan, N. L.; Barron, T. H. K.; Mackrodt, W. C. *Faraday. Discuss.* **1997**, *106*, 377.
(28) Cienfuegos, C.; Isoardi, E. P.; Barrera, G. D. *Phys. Rev. B*, in press.
(29) Allan, N. L.; Barron, T. H. K.; Bruno, J. A. O. *J. Chem. Phys.* **1996**, *105*, 8300.
(30) Gonze, X.; Beuken, J. M.; Caracas, R.; Detraux, F.; Fuchs, M.; Rignanese, G.-M.; Sindic, L.; Verstraete, M.; Zerah, G.; Jollet, F.; Torrent, M.; Roy, A.; Mikami, M.; Ghosez, Ph.; Raty, J. Y.; Allan, D. C. *Comput. Mater. Sci.* **2002**, *25*, 478.
(31) Martin, R. M. *Electronic Structure: Basic Theory and Practical Methods*, Cambridge University Press: Cambridge, U.K., 2004.
(32) Goedecker, S.; Teter, M.; Hutter, J. *Phys. Rev. B* **1996**, *54*, 1703.
(33) Perdew, J. P.; Burke, K.; Ernzerhof, M. *Phys. Rev. Lett.* **1996**, *77*, 3865.
(34) Hartwigsen, C.; Goedecker, S.; Hutter, J. *Phys. Rev. B* **1998**, *58*, 3641.
(35) Gonze, X.; Lee, C. *Phys. Rev. B* **1997**, *55*, 10355.
(36) http://www.isis.rl.ac.uk/molecularspectroscopy/.
(37) Ramirez-Cuesta, A. J. *Comput. Phys. Commun.* **2004**, *157*, 226.
(38) Montanari, B.; Jones, R. O. *Chem. Phys. Lett.* **1997**, *272*, 347.
(39) Montanari, B.; Ballone, P.; Jones, R. O. *J. Chem. Phys.* **1998**, *108*, 6947.
(40) Avitabile, G.; Napolitano, R.; Pirozzi, B.; Rouse, K. D.; Thomas, M. W.; Willis, B. T. M. *J. Polym. Sci., Polym. Lett. Ed.* **1975**, *13*, 351.
(41) Takahashi, Y. *Macromolecules* **1998**, *31*, 3868.
(42) Tashiro, K.; Tanaka, I.; Oohara, T.; Niimura, N.; Fujiwara, S.; Kamae, T. *Macromolecules* **2004**, *37*, 4109.
(43) Shirane, G.; Shapiro, S. M.; Tranquada, J. M. *Neutron Scattering with a Triple-Axis Spectrometer*; Cambridge University Press: Cambridge, U.K., 2002.
(44) Barnes, J.; Fanconi, B. *J. Phys. Chem. Ref. Data* **1978**, *7*, 1309.
(45) Snyder, R. G.; Schachtschneider, J. H. *Spectrochim. Acta* **1965**, *19*, 85.
(46) Olf, H. G.; Fanconi, B. J. *J. Chem. Phys.* **1973**, *59*, 534.
(47) Braden, D. A.; Parker, S. F.; Tomkinson, J.; Hudson, B. S. *J. Chem. Phys.* **1999**, *111*, 429.
(48) Tomkinson, J.; Parker, S. F.; Braden, D. A.; Hudson, B. S. *Phys. Chem. Chem. Phys.* **2002**, *4*, 716.
(49) Takahashi, Y. *Macromolecules* **2001**, *34*, 7836.
(50) Hirata, S.; Iwata, S. *J. Chem. Phys.* **1998**, *108*, 7901.
(51) Parks, W.; Richards, R. B. *Trans. Faraday Soc.* **1949**, 203.
(52) Choy, C. L.; Leung, W. P *J. Polym. Sci., Polym. Phys. Ed.* **1985**, *23*, 1759.
(53) Zhang, M.-L.; Miao, M. S.; Van elsenoy, C.; Ladik, J. J.; Van Doren, V. E. *Solid State Commun.* **2000**, *116*, 339.
(54) Odajima, A.; Maeda, T. *J. Polym. Sci. C* **1966**, *15*, 55.
(55) Auffermann, G.; Barrera, G. D.; Colognesi, D.; Corradi, G.; Ramirez-Cuesta, A. J.; Zoppi, M. *J. Phys.: Condens. Matter* **2004**, *16*, 5731.
(56) Barrera, G. D.; Colognesi, D.; Mitchell, P. C. H.; Ramirez-Cuesta, A. J. *Chem. Phys.* **2005**, *317*, 119−129.

MA052602E